

# On preconditioners for the Laplace double-layer in 2D

Bryan Quaife and George Biros

October 29, 2018

## Abstract

The discretization of the double-layer potential integral equation for the interior Dirichlet Laplace problem in a domain with smooth boundary results in a linear system that has a bounded condition number. Thus, the number of iterations required for the convergence of a Krylov method is, asymptotically, independent of the discretization size  $N$ . Using the Fast Multipole Method (FMM) to accelerate the matrix-vector products, we obtain an optimal  $\mathcal{O}(N)$  solver. In practice, however, when the geometry is complicated, the number of Krylov iterations can be quite large—to the extent that necessitates the use of preconditioning.

We summarize the different methodologies that have appeared in the literature (single-grid, multigrid, approximate sparse inverses) and we propose a new class of preconditioners based on an FMM-based spatial decomposition of the double-layer operator. We present an experimental study in which we compare the different approaches and we discuss the merits and shortcomings of our approach. Our method can be easily extended to other second-kind integral equations with non-oscillatory kernels in two and three dimensions.

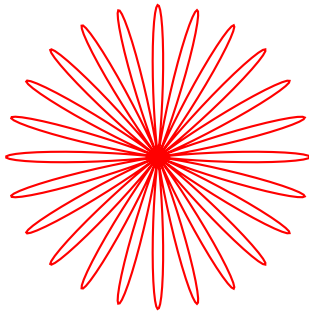
## 1 Introduction

We consider the solution of the interior Laplace equation with Dirichlet boundary conditions in a complex, simply-connected domain  $\Omega$  with smooth boundary  $\Gamma$ , and boundary data  $f$ :

$$\Delta u = 0, \text{ in } \Omega, \quad u = f, \text{ on } \Gamma.$$

Using a double-layer assumption, we formulate the problem as a boundary integral equation (BIE)

$$\eta(\mathbf{x}) + \int_{\Gamma} K(\mathbf{x}, \mathbf{y})\eta(\mathbf{y}) = 2f(\mathbf{x}), \quad \mathbf{x} \in \Gamma \quad \text{or} \quad (I + \mathcal{D})\eta = f, \quad \text{or simply} \quad A\eta = f. \quad (1)$$



$N$	GMRES	<i>Preco</i> GMRES
512	240	9
1,024	228	11
2,048	301	16
4,096	405	20
8,192	626	24
16,382	718	29

Figure 1: To illustrate the difficulties of “inverting” the double-layer potential for a complex geometry consider the boundary depicted on the left. The boundary is  $C^\infty$ , but has high derivatives. Resolving this boundary requires a large number of points even when using a spectrally accurate discretization. (Note that the boundary does not intersect itself in the middle as we can see in the right-most plot of Figure 2.) On the right, we report the number of unpreconditioned and preconditioned GMRES iterations (*Preco*), for tolerance equal to  $10^{-12}$ , as a function of  $N$ , the number of points used to discretize the boundary. We have developed a novel, FMM-based, preconditioner for integral equations (see section 3.3), which we used to compute the results for the preconditioned GMRES. First, notice that despite the fact that we solve a second-kind integral equation, the number of GMRES iterations increases. This is because we have not resolved sufficiently the geometry. (Eventually the number of iterations does become mesh-independent.) Second, by using our FMM-based single-grid preconditioner (with 50 points per leaf) we can significantly decrease the number of GMRES steps and the overall cost of the calculation. In section 4, we will see that using multigrid on this problem does not reduce the overall computational cost, again because the geometry is barely resolved even for  $N = 16,382$ .

for the unknown double-layer density  $\eta(\mathbf{y})$ . Here  $K(\mathbf{x}, \mathbf{y})$  is the double-layer kernel of the Laplacian,  $I$  is the identity operator,  $\mathcal{D}$  is the double-layer potential operator, and the constant 2 has been absorbed in  $f$ .

The discretization of (1) results in a dense unsymmetric system of equations. Gaussian elimination requires  $\mathcal{O}(N^3)$  work where  $N$  is the number of unknowns, which is prohibitively expensive. Since (1) has a bounded condition number [1], a Krylov method like the Generalized Minimum Residual Method (GMRES) [2] coupled with an FMM acceleration [3] for the matrix-vector multiplication (henceforth, “*matvec*”) results in  $\mathcal{O}(N)$  work, which is algorithmically optimal. The constant in this complexity has two factors, one factor captures the FMM matvec costs, and the second one captures the number of GMRES iterations. Here we focus on reducing the latter.

Although the number of GMRES iterations eventually becomes independent of  $N$ , this number can be quite large depending on the complexity of the geometry. (This also implies that in the pre-asymptotic regime the number of iterations can increase quite significantly.) One way to quantitatively characterize the complexity of the geometry is by the number of points  $N$  required to approximate  $D\eta$  accurately enough for  $\eta(\mathbf{x}) = 1(\mathbf{x})$ , the constant density function that is equal to one for all  $\mathbf{x}$ . If  $N$  is large, the solution of (1) will require hundreds or even thousands of GMRES iterations. Such cost makes the solution of (1) prohibitively expensive. The number of iterations becomes even more pronounced for boundaries with corners.

## 1.1 Summary of methodology and contributions

Our goal is to design preconditioners that can be applied to a variety of integral equations with non-oscillatory kernels in two- and three-dimensions, and can be built on top of standard FMM codes. Based on the FMM hierarchical decomposition, we propose a new preconditioner, which we term “*FMMSCHUR*”. To motivate and evaluate the preconditioner, we review existing methods and we provide preliminary comparative results. FMMSCHUR costs  $\mathcal{O}(N \log N)$  work and its construction can be done based on the FMM hierarchy independent of the dimension of the problem. FMMSCHUR is quite effective in reducing the number of GMRES iterations when complex geometries are involved.

FMMSCHUR’s basic idea is to combine a preconditioner for the near-field interactions in the FMM with a two-level low rank approximation of the far-field interactions. In particular it uses the following concepts: Near-far field decomposition, a Schur approximate factorization based on this factorization, and algorithms for low-rank approximation of a matrix.

- The **Near-far field decomposition** of  $D$  is defined as

$$D = D_0 + \sum_{\ell} D_{\ell}.$$

$D_0$  represents the near-field interactions. These also known as *direct* interactions since they are *not* approximated in the FMM.  $D_{\ell}$  represent

different parts of the far field (approximated in the FMM). For example,  $D_1$  corresponds to the first level of the so called  $V$ -list interactions. We make this decomposition precise in section 2.4. Most production integral equation codes use single-grid preconditioning techniques based on approximate factorizations of  $A_0 = I + D_0$ .

- **Schur low-rank.** Given  $A_1 = A_0 + D_1$  and using the FMM factorization of  $D_1$  which can be written as  $D_1 = L_1 M_1^T$ , we can use the Sherman-Morrison-Woodbury (SMW) formula to approximate the inverse of  $A_1$ . The operators  $L_1$  and  $M_1^T$  correspond to the downward pass (translations and local-to-local) and upward pass (multipole-to-multipole) operators in the FMM. Although formally  $D_1$  is not low rank, it is a compact operator can be approximated using a low-rank decomposition (classical FMM is based on this low-rank property). Based on this observation, we can approximate the inverse of  $A_1$  as follows. First we approximate  $A_0^{-1}$ . We use an incomplete LU decomposition with a drop tolerance of  $10^{-3}$ . Then, to invert  $A_1$  using the SMW formula we need to approximate the inverse of  $I + M_1^T A_0^{-1} L_1$ . For this, we will use SMW one more time and we use a low-rank approximation of  $M_1^T A_0^{-1} L_1$ . This approximate inverse significantly reduces the number of GMRES iterations required to invert  $A_1$ . Finally, once this preconditioner of  $A_1$  is formed, we use a rank  $\mathcal{O}(N \log N)$  approximation of  $(A - A_1)$  to complete the construction of FMMSCHUR. This preconditioner can be built on top of standard FMM codes, is not restricted to two-dimensions, and the overall complexity of applying this preconditioner is  $\mathcal{O}(N \log N)$ . These ideas are explained in detail in section 3.3.

Our scheme can be further improved as follows. Classical multigrid for second kind integral equations can be quite effective. In fact for certain problems it is much more efficient than using a more involved scheme like FMMSCHUR. In some other problems it pays off to combine FMMSCHUR with a two-level multigrid. For a given target accuracy in the solution, the discretization size  $N$  is dictated by  $N_f$  required to resolve  $f$  and  $N_\Gamma$  required to resolve  $\Gamma$ . If  $N_f \gg N_\Gamma$  multigrid can be used with the coarse level being the level at which  $N \approx N_\Gamma$ . If  $N_\Gamma \geq N_f$ , multigrid will not help.

The smoothing scheme in multigrid can be either the Picard step, namely  $\eta = f - D\eta$ , or a near-far field splitting iterative method (see section 3). We use a two-grid scheme combined with a spectral projection-based discretization method. The coarse grid solve is done with GMRES preconditioned by FMMSCHUR.

In summary, our method is based on the following formulation and discretization choices.

- We use a spectral discrete Galerkin formulation in which the unknown density  $\eta$  is represented by its Fourier coefficients.
- The boundary integral operator is applied in real space using Nyström integration with the trapezoid rule.

- In the multigrid versions of our preconditioners, the restriction and prolongation operators are spectral projection performed using the FFT (section 2.2). We experimented with other prolongation and restriction operators, but we elected to use spectral methods so that we can best analyze the quality of the smoothers.
- Coarsening of  $D$  in our multigrid versions is done using two alternative methods: projection-based and geometry-based. The former is more effective in reducing the number of GMRES iterations but it does not reduce the overall cost of the calculation. The latter is more efficient computationally as long as the coarse grid operator sufficiently resolves the geometry. (The intergrid transfer operators are the only component that depends on the particulars of the double-layer potential in 2D.)
- In some of our preconditioning schemes we use low-rank approximations of operators. A rank  $p$  approximation is computed by forming the full SVD  $U\Sigma V^*$  and then constructing  $U_p\Sigma_t V_p^*$ , where  $U_p$  contains only the  $p$  columns of  $U$  and  $V_p$  the  $p$  rows of  $V$  that correspond to the  $p$  largest singular values  $\Sigma_p$ . This of course is not a scalable approach. Approximate techniques for such decompositions can be found [4], require only matrix-vector multiplications and are necessary for obtaining the  $\mathcal{O}(N \log N)$  convergence. For simplicity, we have not incorporated such techniques in this initial implementation of FMMSCHUR.
- Our implementation is prototyped in MATLAB so actual run times are uninformative. To assess the performance of the different preconditioners we measure their cost in terms of matvecs with  $D$ .

We consider the following preconditioners: multigrid with Picard smoother, different sparse approximations of  $D$ , and the FMM-based decomposition which involves different levels of the FMM operator. We define a measure of the complexity of the boundary: the number of discretization points required to compute  $\|D_N \mathbf{1}(\mathbf{x}) + \frac{1(\mathbf{x})}{2}\| / \|\mathbf{1}(\mathbf{x})\|$  accurately (using either the  $L^2$ - or the  $L^\infty$ -norm). As mentioned, the effectiveness of the multigrid depends on how accurately  $D_N$  approximates  $D$  on the coarsest grid.

**Contributions.** Our first contribution is a numerical study of the main preconditioning techniques that have appeared in the literature: (i) We test the classical Picard-multigrid method. We examine the effect of approximating the geometry in coarser grids and discuss the effects of using a projection-based versus a geometry-based coarse grid operator. (ii) We consider sparse approximate preconditioners for  $A$  which are based on factorizations of  $A_0 = I + D_0$ . In sparse approximate preconditioners, one typically introduces two approximations. The first approximation is that the far field interactions are dropped and only the near field interactions are used to construct the preconditioner. The second approximation is that the near field interactions are factorized using either incomplete factorizations or some variant of a sparse approximate inverse (SPAI) method. The main trade-offs in constructing such preconditioners are the computational cost of constructing and applying the preconditioner,

its effectiveness, and its parallelizability. Here we only consider the issue of effectiveness. To assess it, we consider block diagonal, banded, incomplete, and exact factorizations of the near field. We provide numerical examples that show that such an approximation reduces the number of iterations, but the overall speed-up may be less than a factor of two.

Our second and main contribution is to introduce FMMSCHUR a new preconditioning scheme that includes the far interactions in the preconditioner. Our scheme is based on the FMM hierarchy and a sequence of low-rank approximations combined with the SMW identity. It resembles the structure of the fast direct solvers [5]. It uses a different spatial decomposition which is directly related to the FMM. It does not lead to an exact factorization but it can be easily built on top of an FMM scheme. Experimentally we see a tenfold reduction on the number of GMRES iterations. We estimate that the cost of the preconditioner will be equivalent to two matvecs, so the expected overall speedup will be a factor of five. We provide numerical evidence that this preconditioner performs well even when we use a very low-order approximation of the far field in the preconditioner.

## 1.2 Previous Work

Already in the 60's and 70's, there were attempts to design efficient iterative solvers for “inverting”  $I + D$ . These efforts continue up to now with research on preconditioners and direct solvers. There have been many approaches based on two-grid and multigrid solvers, fixed point iterations, approximate factorizations of the near field interactions, analytic preconditioners, and low-order-FMM self-preconditioning approaches. Our discussion below is by no means exhaustive but, we hope, summarizes the main methodologies for preconditioning the double-layer operator.

Multigrid methods [6, 7, 8, 9] were one of the first attempts at constructing efficient solvers for  $I + D$ . The main concerns were the choice of the smoothers and the robustness of the method for Nyström discretizations. The ingredients for constructing a multigrid scheme are a Picard iteration as a smoother along with restriction and prolongation using either injection and Nyström interpolation or a standard  $L^2$ -projection. Further research on multigrid methods extended their applicability to polygonal domains, high-order piecewise polynomial Galerkin discretizations, and problems in three dimensions (see [10] and the references there in). The geometries examined were typically quite simple (spheres, ellipsoids, polygonal domains with a small number of corners). We will see that such methods are indeed optimal, assuming that the coarse grid resolves the geometry and can be computed inexpensively. But in many practical cases this is not the case.

Since the coarse grid solve may not be cheap for complex geometries, there has been a lot of work on preconditioning integral equations using single-grid methods, mainly approximate factorizations. It was quickly recognized that the most natural approach is to approximately factorize  $D_0$ , the direct-interaction part of FMM that corresponds to a sparse matrix. But exactly factorizing  $D_0$

is too expensive using current technologies. In [11], the authors consider a preconditioner based on near interactions of the FMM that resembles a block factorization but retains some off-block interactions; they apply it successfully to first-kind integral equations. The same preconditioning idea is used in [12], in which the authors combine it with a self-preconditioning scheme in which  $I + D$  is preconditioned with a low-order approximation [13] of the operator  $D$ , combined with an approximate sparse factorization similar to that of [11]. The preconditioner somewhat reduces the number of GMRES iterations but the overall wall-clock time does not significantly improve over the unpreconditioned case since inverting the low-order matrix  $I + D$  is also quite expensive.

The ideas of approximate sparse factorizations of the near field interactions are further explored by Chen [14] in which banded, block, and sparse approximate inverse (SPAI) factorizations are discussed. In the latter, the basic idea of constructing a preconditioner is to assume a sparsity structure for the preconditioner and solve for each column of the preconditioner by solving several small least-squares problems. It was found that the banded approximation is not efficient unless the band width approaches the full width of the matrix. For the sparse approximate inverse, one difficulty is to find a good sparsity pattern. Band patterns are used for problems in one and two dimensions (an ellipse) and a cylinder in three dimensions. More complex geometries were not discussed. In [15], the SPAI ideas are further pursued in trying to discover a proper sparsity and truncation (for the least-squares problem) based on the near interactions constructed by the FMM and combine them to design a parallel preconditioner. Their preconditioner is based on Frobenius-norm minimization with a pattern prescribed in advance. They solve an extremely challenging problems, 3D Helmholtz problems in complex geometries (aircraft), and combine the SPAI preconditioner with the inner-outer iteration of Grama et al. [12], but it is unclear that the use of the preconditioner results in significant computational savings.

Other approaches for preconditioners include incomplete LU (ILU) factorizations [16], and analytic preconditioners [17] in which the solution of a regular geometry for which the inverse is known analytically is used to precondition the operator on an arbitrary simply-connected geometry.

An alternative to iterative methods is to use a direct method. Of course this is expensive, so approximate direct methods have been developed for both integral equations and generic sparse matrices [5, 18, 19, 20]. These methods are similar to nested dissection and domain decomposition methods and they rely not on sparsity, but on the fact that if the boundary of the BIE is decomposed into two pieces, each side can be solved with only a low-rank update coming from the other side. This is applied recursively to form a compressed version of the inverse in  $\mathcal{O}(N^{3/2})$  time for highly complex geometries. For simple geometries like an ellipsoid, the construction cost becomes  $\mathcal{O}(N \log N)$ . While this is more expensive than GMRES coupled with the FMM, this compressed inverse can be applied in  $\mathcal{O}(N \log N)$  time with a small constant. Therefore, for problems that involve multiple right-hand sides for the same matrix, fast direct solvers are quite effective.

Finally, in the context of multiply-connected geometries, which we do not consider here, in [21] the authors use a Picard preconditioner that is modified to help reduce the additional iterations that GMRES requires to resolve the extra equations that arise from the multiply-connectedness of the geometry. They do not consider this preconditioner in a geometric multigrid setting and while they consider geometries that are up to 200-ply connected, each component curve is an ellipse with aspect ratio no greater than three.

In summary, the bulk of the literature can be perhaps roughly categorized in three classes of solvers. One is to accelerate fixed point schemes using grid hierarchies. The second is to accelerate GMRES using some type of sparse factorization based on the near field. Finally, the recent efforts in fast direct solvers are promising for the case of multiple right-hand sides but so far seem to have a superlinear construction phase.

### 1.3 Limitations

Our methodology is by no means complete. It requires the exact or approximate factorization of the near field  $I + D_0$ , whose computation we do not investigate here. Such a factorization could be computed using recent methods for fast factorization of sparse matrices [19, 22]. Unlike fast direct solvers, our method is approximate and we cannot prove algorithmic costs, since, for example, we cannot bound the number of GMRES iterations.

We consider a straightforward problem, the simply-connected interior Laplace problem in 2D with smooth geometries to isolate the geometry effects. Extensions of the proposed methodology in three dimensions, geometries with corners, and more difficult operators like the Helmholtz problem will require further work. Several aspects of our scheme require low-rank properties that do not directly extend to oscillatory Helmholtz problems.

The coarse grid points are chosen by a simple filtering of the fine grid. An adaptive discretization using a smaller number of unknowns could possibly extend multigrid methods to much more complex geometries. Such representations will require more generic (than spectral) intergrid operators. We have not considered such cases here.

Finally, a more thorough analysis of the preconditioners and smoothers is also required, but this is difficult to do for arbitrary geometries especially since we are interested in the actual constants in the complexity estimates.

### 1.4 Organization of the paper

In section 2 we summarize the discretization, the structure of the FMM, the decomposition into near and far fields, the intergrid transfer operators, and the coarse grid operators. In section 3 we define the different preconditioning techniques, and in section 4 we discuss the results.



## 2 Formulation

Notation	Descriptions
BIE	Boundary integral equation
FMM	Fast multipole method
GMRES	Generalized minimum residual method
SMW	Sherman-Morrison-Woodbury identity
SVD	Singular value decomposition
$\mathcal{D}$	Double-layer potential integral operator
$\kappa$	Curvature
$\mathbf{n}$	Unit outward normal
$K(\mathbf{x}, \mathbf{y})$	Kernel of the double-layer potential
$N$	Number of points on the finest grid
$N_{\min}$	Number of points on the coarsest grid
$D_N$	$N$ -point discretization of $\mathcal{D}$
$m$	Number of GMRES iterations
$m_{coarse}$	Number of GMRES iterations on the coarsest grid
$s$	Maximum number of points in each leaf
$U$ -list	The set of boxes that neighbor a leaf node
$V$ -list	The set of children of the neighbours of a box's parent that are not neighbours themselves

Table 1: Frequently used acronyms and symbols.

Boundary Integral Equations (BIEs) are a reformulation of boundary value problems that have the advantage of only having to discretize the boundary of the physical domain. This reduces the dimension of the problem by one and allows for complex domains. Here we formalize the problem of interest and set notation. Let  $\Omega \subset \mathbb{R}^2$  be a bounded, simply-connected, domain with smooth boundary  $\Gamma$ . The geometries that we will consider are  $\mathbf{x}(\theta) = (cr(\theta)\cos(\theta), r(\theta)\sin(\theta))$ ,  $0 \leq \theta < 2\pi$ , where

$$\textit{Simple} : r(\theta) = 0.5(\cos^2(\theta) + 9\sin^2(\theta))^{1/2} + 0.07\cos(12\theta), c = 0.85,$$

$$\textit{Moderate} : r(\theta) = 1 + 0.5\cos(3\theta) + 0.05\cos(30\theta), c = 1,$$

$$\textit{k-lobed Flower} : r(\theta) = 1 + 0.98\cos(k\theta), c = 1.$$

Figure 2 illustrates these geometries that we are considering. Consider the boundary value problem

$$\Delta u = 0, \mathbf{x} \in \Omega, \quad u = g, \mathbf{x} \in \Gamma. \quad (2)$$

Using the fundamental solution  $-\frac{1}{2\pi} \log |\mathbf{x}|$  of (2), we seek a solution in the form

$$u(\mathbf{x}) = -\frac{1}{2\pi} \int_{\Gamma} \frac{\partial}{\partial \mathbf{n}_{\mathbf{y}}} \log |\mathbf{x} - \mathbf{y}| \eta(\mathbf{y}) ds_{\mathbf{y}}, \quad \mathbf{x} \in \Omega, \quad (3)$$

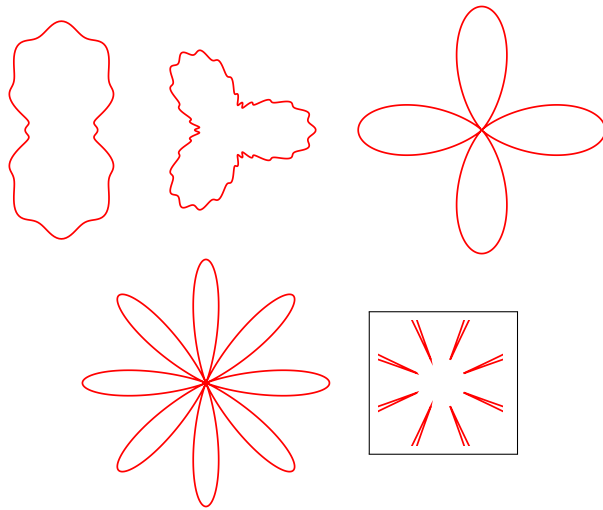


Figure 2: Four different geometries that we use to demonstrate the abilities and limitations of our methods. From left to right, the geometries are as follows. *Simple*: The curvature changes from  $-27$  to  $17$  at the two rapidly changing locations, and with  $N = 128$  the discretization error is  $1.3 \times 10^{-6}$ . *Moderate*: The curvature ranges from  $-188$  to  $136$ , and with  $N = 256$  the discretization error is  $7.2 \times 10^{-3}$ . *Four-lobed Flower*: The curvature ranges over four orders of magnitude and  $N = 2048$  gives a discretization error of  $5.4 \times 10^{-3}$ . *Eight-lobed Flower*: The curvature ranges over six orders of magnitude and  $N = 4096$  gives a discretization error of  $7.9 \times 10^{-2}$ . The final plot is a 40 times magnification of the center of the eight-lobed flower.

where  $\mathbf{n}_y$  is the unit outward normal to  $\Gamma$  at  $\mathbf{y}$ . The ansatz (3) is called the double-layer potential and we write  $u(\mathbf{x}) = \mathcal{D}[\eta](\mathbf{x})$ . The function

$$K(\mathbf{x}, \mathbf{y}) = -\frac{1}{2\pi} \frac{\partial}{\partial \mathbf{n}_y} \log |\mathbf{x} - \mathbf{y}|$$

is called the kernel of the integral operator, and its limiting value is

$$\lim_{\substack{\mathbf{y} \in \Gamma \\ \mathbf{y} \rightarrow \mathbf{x}_0}} K(\mathbf{x}_0, \mathbf{y}) = \frac{1}{4\pi} \kappa(\mathbf{x}_0), \quad (4)$$

where  $\kappa(\mathbf{x}_0)$  is the curvature at  $\mathbf{x}_0 \in \Gamma$ . To satisfy the boundary data of (2),  $\eta$  must satisfy the Fredholm integral equation of the second kind [23, 24, 25]

$$g(\mathbf{x}_0) = \frac{1}{2} \eta(\mathbf{x}_0) + \mathcal{D}[\eta](\mathbf{x}_0), \quad \mathbf{x}_0 \in \Gamma.$$

By defining  $f = 2g$  and absorbing the 2 into the double-layer potential, we need to solve

$$f(\mathbf{x}_0) = \eta(\mathbf{x}_0) + \mathcal{D}[\eta](\mathbf{x}_0), \quad \mathbf{x}_0 \in \Gamma. \quad (5)$$

Since the kernel  $K$  is bounded, the integral operator  $\mathcal{D}$  is compact and the Fredholm alternative guarantees the existence and uniqueness of solutions of (5).

## 2.1 Discretization

To discretize (5), we let  $\mathbf{x}(\theta)$  be a parameterization of  $\Gamma$  and discretize  $\Gamma$  at  $\{\mathbf{x}(\theta_j) \mid \theta_j = (j-1)2\pi/N, j = 1, \dots, N\}$ . We let  $\mathbf{f}_j = \mathbf{f}(\mathbf{x}(\theta_j))$  and use similar notation for the other variables. The resulting linear system is

$$\mathbf{f}_j = \boldsymbol{\eta}_j + \sum_{k=1}^N K_{jk} \boldsymbol{\eta}_k, \quad j = 1, \dots, N, \quad \text{or} \quad \mathbf{f} = (I + D_N) \boldsymbol{\eta}, \quad (6)$$

where  $K_{jk} = 2K(\mathbf{x}_j, \mathbf{x}_k) |\Delta \mathbf{s}_k|$ , and  $\Delta \mathbf{s}$  is the Jacobian. Equation (4) is used for the diagonal terms  $K_{jj}$ . Equation (6) can be interpreted as a Fourier projection method since the  $N$ -point trapezoid rule integrates the first  $N$  Fourier frequencies exactly. That is, if we let  $F_N^T$  denote the  $N$ -point Fourier projection and let  $F_N$  be its inverse, then (6) is equivalent to

$$F_N^T (I + D_N) F_N F_N^T \boldsymbol{\eta}_N = F_N^T \mathbf{f}_N.$$

This motivates using Fourier restriction and prolongation operators which we define in the next section.

Since (5) is a second-kind BIE (it would be of the first kind if the term  $\eta(\mathbf{x}_0)$  was not present), we are guaranteed that  $m$  is bounded independent of  $N$ . The number of required GMRES iterations,  $m$ , depends only on the complexity of  $\Gamma$ . In Table 2, we consider ellipses with different aspect ratios,

and in Table 3 we consider the flower-shaped geometry (see Figure 2) with different numbers of lobes. We see that the largest curvature has a slight affect on the number of GMRES iterations but it is the number of high curvature points that substantially increases  $m$ . However, given a fixed geometry, once  $N$  is sufficiently large that the geometry is resolved, mesh independence is observed from this point onwards.

Aspect Ratio	$m$	Number of Lobes	$m$
2	3	2	28
4	4	3	44
8	7	4	53
16	10	5	90
32	13	6	91
64	15	7	127
128	17	8	171

Table 2: The number of required GMRES iterations to achieve a tolerance of  $10^{-12}$  for ellipses of varying aspect ratios. We see that the aspect ratio has a small role on the number of GMRES iterations.

Table 3: The number of required GMRES iterations to achieve a tolerance of  $10^{-12}$  for a flower-shaped geometry with a varying number of lobes. We see that the number of points of high curvature has an important role on the number of GMRES iterations.

## 2.2 Restriction and Prolongation

We introduce the spectral prolongation  $P$  and restriction  $R$  operators. Restriction is done by taking the Fourier transform, truncating the tail of the spectrum, and then computing the inverse Fourier transform. Mathematically, if  $\mathbf{f} \in \mathbb{C}^N$  is represented as

$$\mathbf{f}_j = \sum_{k=-N/2}^{N/2-1} \hat{f}_k e^{ik\theta_j}, \quad \theta_j = (j-1) \frac{2\pi}{N}, \quad j = 1, \dots, N,$$

then the restriction of  $\mathbf{f}$  is

$$(R_N^{N/2} \mathbf{f})_j = \sum_{k=-N/4}^{N/4-1} \hat{f}_k e^{ik\theta_j}, \quad \theta_j = (j-1) \frac{4\pi}{N}, \quad j = 1, \dots, N/2.$$

Similarly, if  $\mathbf{f} \in \mathbb{C}^{N/2}$  is represented as

$$\mathbf{f}_j = \sum_{k=-N/4}^{N/4-1} \hat{f}_k e^{ik\theta_j}, \quad \theta_j = (j-1) \frac{4\pi}{N}, \quad j = 1, \dots, N/2,$$

then the prolongation of  $\mathbf{f}$  is

$$(P_{N/2}^N \mathbf{f})_j = \sum_{k=-N/4}^{N/4-1} \hat{f}_k e^{ik\theta_j}, \quad \theta_j = (j-1) \frac{2\pi}{N}, \quad j = 1, \dots, N.$$

### 2.3 Coarse Grid Operators

To use a multigrid method, we also need to construct the double-layer potential  $D$  on coarser grids. We will test two common methods of constructing these operators. The first method is geometry-based. It uses  $R$  to coarsen  $\Gamma$  and then constructs  $D$  using (6). The second method is projection-based. Given the fine grid operator  $D_N \in \mathbb{R}^{N \times N}$ , the coarse grid operator for  $M < N$  is

$$D_M = R_N^M D_N P_M^N.$$

The projection-based coarse grid operator is more accurate, however, it is not practical for large problems since the coarse grid operators require calculations on the finest grid. Since we are using Fourier based restriction and prolongation, we always let  $N/M$  be a power of 2.

### 2.4 Fast Multipole Method

The Fast Multipole Method (FMM), first introduced by Greengard and Rokhlin in [3], is a hierarchical method that can apply the matrix-vector multiplication in (6) with  $\mathcal{O}(N)$  operations. We briefly highlight the components of the FMM that are relevant to our work. Given a discretization of  $\Gamma$ , we form a quadtree so that no leaf contains more than  $s$  points. Our implementation handles adaptive quadtrees (see Figure 3), but to minimize complex definitions, we only present the formulation for uniform quadtrees.

We start by defining two boxes as being neighbours if they share at least one corner or one edge. We say that a box is a neighbour of itself. Given a leaf  $b$  in the quadtree, we let  $P(b)$  be its parent. Then, we divide the quadtree into multiple regions: the  $U$ -list and the  $V_i$ -lists. The  $U$ -list is the set of neighbors that are adjacent to  $b$ , and the  $V_1$ -list is the set of children of  $P(b)$ 's neighbours that are not neighbors of  $b$  (see Figure 4). We write  $U$  for the set of boxes in the  $U$ -list,  $V_1$  for the set of boxes in the  $V_1$ -list,  $V_2$  for the set of boxes in the  $V_1$ -list of  $P(b)$ , etc. Also, we define  $T(B)$  to be the set of points in the set of boxes  $B$ .

Given a vector  $\boldsymbol{\eta}$ , we decompose the evaluation of  $D\boldsymbol{\eta}$  as

$$\begin{aligned} (D\boldsymbol{\eta})_j &= \sum_{k=1}^N K_{jk} \boldsymbol{\eta}_k = \sum_{\mathbf{x}_k \in T(U)} K_{jk} \boldsymbol{\eta}_k + \sum_{\mathbf{x}_k \in T(V_1)} K_{jk} \boldsymbol{\eta}_k + \sum_{\mathbf{x}_k \in T(V_2)} K_{jk} \boldsymbol{\eta}_k + \dots \\ &= (D_0 \boldsymbol{\eta})_j + (D_1 \boldsymbol{\eta})_j + (D_2 \boldsymbol{\eta})_j + \dots \end{aligned}$$

In Figure 5, we illustrate the set of points in the summations for an adaptive tree structure. The adaptivity changes the definitions of  $V_1, V_2, \dots$ . However, to

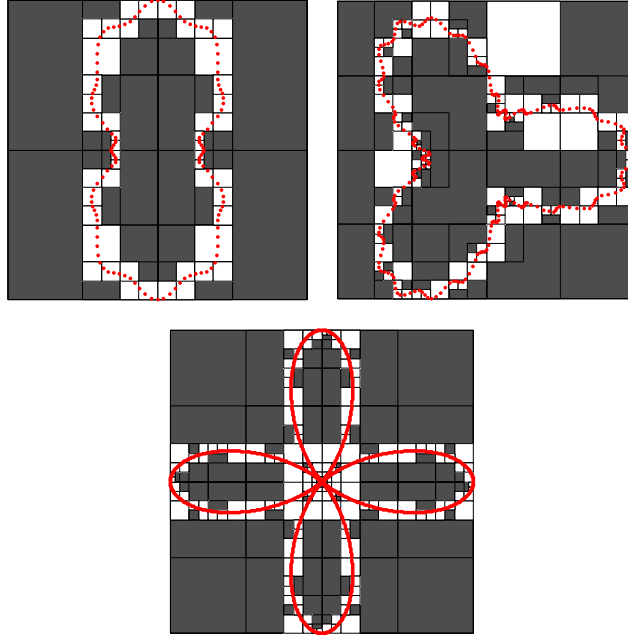


Figure 3: The quadtrees for three of the geometries we introduced in Figure 2. In the left two plots, each leaf contains no more than 4 points. In the right plot, each leaf contains no more than 10 points. Darkened regions contain no points and are removed from the calculation.

$V_1$	$V_1$	$V_1$	$V_1$	$V_1$	$V_1$
$V_1$	$V_1$	$V_1$	$V_1$	$V_1$	$V_1$
$V_1$	$U$	$U$	$U$	$V_1$	$V_1$
$V_1$	$U$	<b><math>b</math></b>	$U$	$V_1$	$V_1$
$V_1$	$U$	$U$	$U$	$V_1$	$V_1$
$V_1$	$V_1$	$V_1$	$V_1$	$V_1$	$V_1$

Figure 4: The  $U$ -list and  $V_1$ -list of box  $b$ . The parent box  $P(b)$  is in bold. The boxes that are not illustrated are in  $V_2, V_3, \dots$

avoid introducing additional notation, we do not redefine these sets and refer the reader to Figure 5 to visualize the different sets. The summation due to points in  $U$ , shown in the left two plots, is denoted by  $D_0$ . Here we have made a distinction between  $b$  and its other neighbours. This will play a role when we introduce our preconditioners. The summation due to the points in  $V_1$ , shown in the third plot, is denoted by  $D_1$ . The summation due to the points in  $V_2$ , shown in the final plot, is denoted by  $D_2$ .

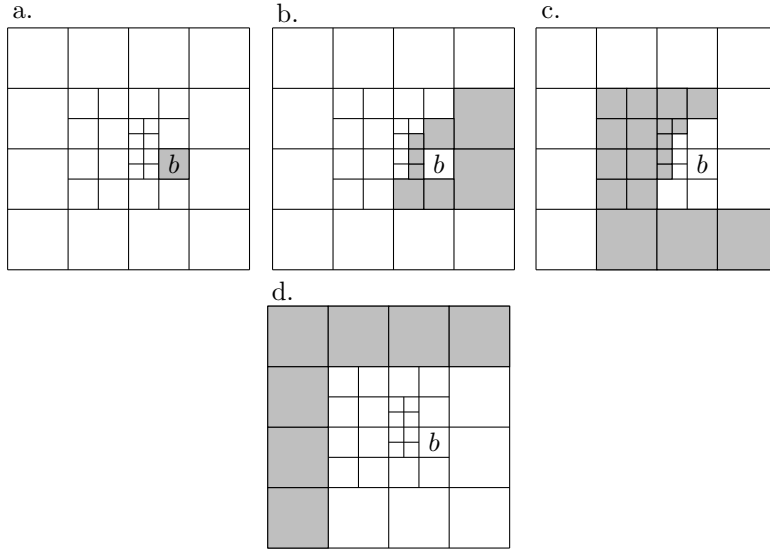


Figure 5: For points inside box  $b$ , the layer potential  $D$  is approximated with points in a set of neighboring boxes. a.  $D_0$ : Box  $b$ ; b.  $D_0$ : Boxes in  $U$ ; c.  $D_1$ : Boxes in  $V_1$ ; d.  $D_2$ : Boxes in  $V_2$ .

The key idea of the FMM is methods for approximating the far field. The matrices  $D_\ell, \ell \geq 1$  can be approximated by a factorization of the form

$$D_\ell = L_\ell T_\ell M_\ell^T.$$

$M_\ell^T$  represents building the multipole moments (or the equivalent densities for kernel-independent methods [26, 27]),  $T_\ell$  represents translation operators that transform multipole coefficients to polynomial coefficients, and  $L_\ell$  represents the downward traversal of a tree. For the rest of the paper we absorb  $T_\ell$  in  $L_\ell$  so that  $D_\ell = L_\ell M_\ell^T$ .

$L_\ell, M_\ell$  can be approximated efficiently in the FMM to result in an  $\mathcal{O}(N)$  scheme. So,  $D_\ell$  is an  $N \times N$  matrix and can be approximated very well by  $L_\ell M_\ell^T$ , where  $L_\ell, M_\ell \in \mathbb{R}^{N \times m_\ell}$ . For example, if we use  $s$  points per box and we use  $p$  multipole moments as we traverse the tree,  $m_\ell = p \frac{N}{s^{4^\ell - 1}}$ .

### 3 Preconditioners

In this section, we introduce several strategies for solving and preconditioning (6). We focus mainly on single-grid preconditioners.

#### 3.1 Picard

The simplest iterative method for solving (6) is using the Picard iteration

$$\boldsymbol{\eta}^{\text{new}} = \mathbf{f} - D\boldsymbol{\eta}^{\text{old}}. \quad (7)$$

The Picard iteration (7) is not convergent since standard potential theory [24] shows that  $\mathcal{D}[1](\mathbf{x}) = 1$ . Therefore, as  $N \rightarrow \infty$ , the spectral radius of  $D$  approaches 1 and (7) is only stable. Of course (7) is not being used as an iterative solver. Instead, it is used as a smoother [1, 7, 28, 29] in a multigrid scheme.

By coupling this smoother with the previously discussed prolongation, restriction, and coarse grid operators, a multigrid algorithm is formed. Multigrid can then be used as a solver for (6). However, it is more efficient to use it as a preconditioner for GMRES. Unfortunately, using the Picard smoother when the coarse grid is not sufficiently resolved results in a multigrid algorithm that can slow down the convergence of GMRES.

#### 3.2 Near-Far Field Splitting

Another iterative method for solving (6) is formed by first splitting  $D$  into a near field and a far field. Single-grid preconditioners can be derived by the FMM decomposition  $D = D_{\text{near}} + D_{\text{far}}$ , where  $D_{\text{near}}$  is the double-layer potential due to the near field and  $D_{\text{far}}$  is the double-layer potential due to the far field. We can iterate on the equation

$$(I + D_{\text{near}})\boldsymbol{\eta}^{\text{new}} = \mathbf{f} - D_{\text{far}}\boldsymbol{\eta}^{\text{old}}. \quad (8)$$

This scheme can be either used as a smoother or we can use it as a single-level preconditioner (with  $\boldsymbol{\eta}^0 = 0$ ). In the latter case, we simply use

$$P = (I + D_{\text{near}})^{-1},$$

where the inverse indicates either an exact or an approximate factorization. In multigrid this preconditioner can be combined with (8) to define an inexact smoothing step:

$$\boldsymbol{\eta}^{\text{new}} = P(\mathbf{f} - D_{\text{far}}\boldsymbol{\eta}^{\text{old}}).$$

All the preconditioners we define below can be used in a similar manner as approximate smoothers.

We describe several of the options for approximating  $(I + D_{\text{near}})^{-1}$ .



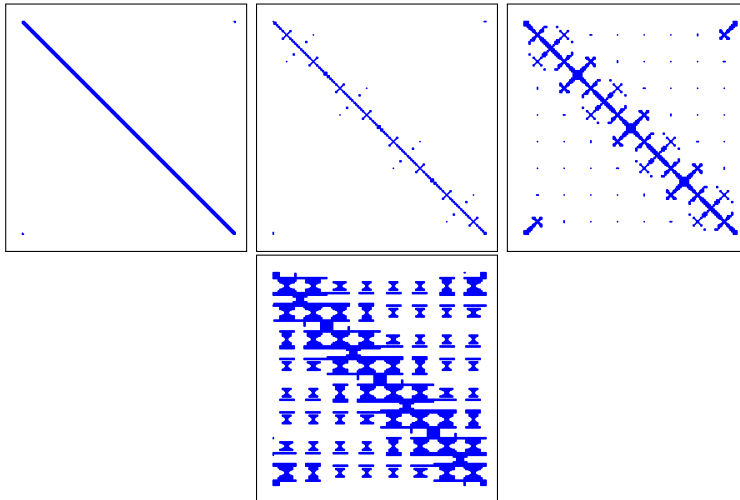


Figure 6: Sparsity plots of  $D_{\text{near}}$  for four different preconditioners. For these plots, we used the eight-lobed flower from Figure 2. The left plot corresponds to the banded approximation  $P_B$ , the second plot corresponds to the block diagonal approximation  $P_D$ , the next plot corresponds to the  $U$ -list approximation  $P_0$ , and the final plot corresponds to the  $V_1$ -list approximation  $P_1$ . The small protrusions from the diagonal of the block diagonal approximation correspond to the eight points where the lobes of the flower approach one another. In the third plot, we can see that the sparsity pattern of  $D_0$  becomes quite complex. A generic fast solver for such matrices is something we are currently investigating. The sparsity pattern of the final plot is far too complex to construct exact inverses.

- $P_B$ , **Banded approximation**: If  $\Gamma$  is not too extreme (left two figures of Figure 2), then we can say that the first  $s$  points to the right and left of each point are in the near field. The sparsity pattern of  $D_{\text{near}}$  is in the left plot of Figure 6.  $P_B$  is very easy to compute and parallelize.
- $P_D$ , **Block diagonal approximation**: Alternatively, we can construct a quadtree and define  $D_{\text{near}}$  to be the double-layer potential due to the set of points in the same leaf  $b$  as the target point. The sparsity pattern of  $D_{\text{near}}$  is illustrated in the second plot of Figure 6 (this matrix is block diagonal after a permutation of the rows). Since  $P_D$  is block diagonal, it is very easy to compute and parallelize.
- $P_0$ ,  **$U$ -list approximation**: We can include more terms from the FMM in  $D_{\text{near}}$ . We remind the reader that the operators  $D_0, D_1, D_2, \dots$  are the double-layer potential due to points in  $U, V_1, V_2, \dots$ , respectively. The simplest case is to use

$$P_0 \approx A_0^{-1} = (I + D_0)^{-1},$$

where  $D_0$  corresponds to the direct interactions in FMM. In the third plot of Figure 6, we illustrate the sparsity of  $I + D_0$ .  $P_0$  is harder to compute and parallelize. It requires fast sparse direct solvers.

- $P_\ell$ ,  **$V_\ell$ -list approximation**: We can include increasingly more and more interactions by using the  $V_\ell$ -list interactions. For example  $P_1 \approx (A_0 + D_1)^{-1}$ . The difficulty of constructing this preconditioner is even higher since  $D_1$  is never constructed but rather is approximated in the FMM scheme. The sparsity pattern of  $A_0 + D_1$  is in the right plot of Figure 6.
- $P_{S,\ell}$ , **FMMSCHUR of  $P_\ell$** : This preconditioner approximates  $P_\ell$  using low-rank decompositions and the SMW formula. It is described in detail in the next section.

These preconditioners can be used as smoothers in a classical V-cycle multi-grid scheme in which the restriction and prolongation operations are done spectrally. We give more details in section 4. More complicated smoothers could be built by using these preconditioners in a splitting-based Picard or Chebyshev iterative scheme. However, the overall cost increases too much, and Chebyshev smoothers require knowledge of the spectrum of  $D$ .

As we mentioned in the introduction, a lot of effort has been put into finding good approximations for  $P_0$ . However, as we will see, even if we use an exact factorization of  $(I + D_0)$  for  $P_0$ , we still require a lot of GMRES iterations. What we have left out is significant. Adding additional levels of interactions to build  $P_1$  and  $P_2$  cannot be done using existing technologies. Next we describe

a new scheme, which we refer to as FMMSCHUR, to build approximations that include additional interactions. Our scheme requires the existence of an efficient approximation for  $P_0$ . The new preconditioner is termed  $P_{S,L}$  and it is a single-grid preconditioner.

### 3.3 Recursive low-rank approximation preconditioner

Recall that we have to invert  $A = I + D$ ,  $A \in \mathbb{R}^{N \times N}$ . Also recall the SMW formula

$$(B + UV)^{-1} = (I - B^{-1}US^{-1}V)B^{-1}, \quad \text{where } S = I + VB^{-1}U.$$

First we will consider an approximation for  $P_1$ . Define  $A_1 = A_0 + D_1$  and assume that  $D_1$  is factorized as  $D_1 = L_1M_1^T$ , where  $L_1, M_1 \in \mathbb{R}^{N \times m_1}$ , where  $m_1 < N$ . In general,  $m_1$  is too large to construct an efficient preconditioner. However, we will see in section 4 that taking  $m_1 = 5$  results in a good preconditioner of  $A_1$ , even though it is a poor approximation of  $P_1$ . Using the SMW formula we can directly write this approximate inverse of  $A_1$

$$A_1^{-1} \approx (I - A_0^{-1}L_1S_1^{-1}M_1^T)A_0^{-1},$$

where  $S_1 = I + M_1^T A_0^{-1} L_1$  with  $S_1 \in \mathbb{R}^{m_1 \times m_1}$ .

This preconditioner requires applying  $S_1^{-1}$  and  $A_0^{-1}$ . Since  $A_0$  is sparse, we compute  $A_0^{-1}$  in linear time with the incomplete LU decomposition. As is for the case for  $D_1 = L_1M_1^T$ , a rank  $m_1 = 5$  approximation of the matrix  $M_1^T P_0 L_1 \approx UV$  results in a good preconditioner of  $S_1$

$$\tilde{S}_1^{-1} = I - U(I + VU)^{-1}V.$$

Combining all the pieces, we have constructed the preconditioner for  $A_1$

$$P_{S,1} = (I - P_0 L_1 \tilde{S}_1^{-1} M_1^T) P_0, \quad (9)$$

where  $P_0$  and  $\tilde{S}_1^{-1}$  are preconditioners for  $A_0$  and  $S_1$ , respectively. Note that applying this preconditioner requires applying  $P_0$  twice.

The cost of constructing  $\tilde{S}_1^{-1}$  depends on how we compute the low-rank approximation of  $M_1^T P_0 L_1$ . Using techniques discussed in [4], the low-rank vectors can be approximated in work that is proportional to the work of applying  $P_0$ . These techniques for forming the require low-rank approximations are left as future work, and in this work, we simply use the truncated SVD.

Now consider the case of  $A_2 = A_1 + D_2$ . The scheme can be applied recursively in which the approximate factorization of  $A_1$  described above can be used to build a preconditioner for  $A_2$

$$P_{S,2} = (I - P_{S,1} L_2 \tilde{S}_2^{-1} M_2^T) P_{S,1},$$

where  $\tilde{S}_2^{-1} \approx (I + M_2^T P_{S,1} L_2)^{-1}$ ;  $\tilde{S}_2^{-1}$  is built by computing a low-rank approximation of  $M_2^T P_{S,1} L_2$ . Applying this preconditioner requires four applications of

$P_0$ . This scheme can be used recursively to add more levels. The main observation is that in our scheme  $D_\ell$  has a smaller norm and stronger compactness than  $D$  since it only involves the far field and no kernel singularities. So the Schur complements  $S_\ell = I + R_\ell$  will be very well-conditioned matrices, with  $R_\ell$  admitting low-rank approximations that can be used to construct good single-grid preconditioners.

Unfortunately, if we use recursion, the cost of applying  $P_{S,L}$  is  $2^L$  times the cost of applying  $P_0$ . Since  $L = \mathcal{O}(\log_4(N/s))$  in 2D, the cost of applying  $P_{S,L}$  is  $\mathcal{O}(N^{3/2})$ . Therefore we need to consider either alternative algorithms that do not apply  $P_{S,L}$  recursively or use small  $L$ , say  $L = 1$ . In this paper we only consider the latter case. If we use small  $L$ , the preconditioner can be further improved by approximating the effect of all other levels by a global low-rank approximation. That is, we write

$$A = A_0 + \sum_{i=1}^L D_\ell + Z.$$

We build  $P_{S,L}$  to approximate the inverse of  $A_0 + \sum_{i=1}^L D_\ell$  and we use a low-rank approximation of  $Z$ , which we combine with  $P_{S,L}$  using the SMW formula. The number of vectors used in approximating  $Z$  is selected so that the cost of applying  $P_{S,L}$  is  $\mathcal{O}(N \log N)$ ; we choose it to be  $\mathcal{O}(\log N)$ . In the next section we provide experimental evidence that using  $L = 1$  with a  $\mathcal{O}(\log N)$ -rank approximation of  $Z$  works quite well.

To see the connection to the FMM, recall the derivation of the SMW formula is based on introducing auxiliary unknowns and using a Schur complement decomposition. Indeed if we want to solve  $(A + D_1)\boldsymbol{\eta} = f$ , we set  $\boldsymbol{\eta}_1 = M_1^T \boldsymbol{\eta}$  and solve a Schur complement for  $\boldsymbol{\eta}_1$  instead of the original system. In the FMM context,  $\boldsymbol{\eta}_1$  corresponds to the multipole moments  $M_1^T \boldsymbol{\eta}$ . For this reason we use the subscript ‘‘S’’ to indicate that it is based on Schur complement decomposition.

As mentioned in the introduction, this preconditioner is different than the fast algorithms for integral equations. Roughly speaking, those are based on non-overlapping Schur decompositions of the domain combined with specially constructed low-rank approximations of the interface and tailored to boundary integral equations. Our scheme is less powerful but can be implemented relatively easily on top of a standard FMM evaluation.

## 4 Results

We discuss the behavior of the different preconditioners in the context of single-grid and multigrid schemes. We conduct a series of experiments, which we now summarize.

- **Single-grid and two-level multigrid** (Table 4): Here we compare the effectiveness of the preconditioners in a single-grid and a two-grid scheme

applied to several geometries. In the single-grid case the new FMM-based preconditioners are more effective. We see that if the coarse grid is sufficiently resolved, then the Picard and  $P_0$  preconditioners work best.

- **Geometric versus projection coarsening** (Tables 5–8): Here we compare the cost of the two methods for creating the coarse grid operators. The projection-based coarse grid operator uses fewer GMRES steps, but it requires too many matvecs. We again see the effect of using unresolved coarse grids. Also, the simpler preconditioners  $P_B$  and  $P_D$  do not reduce the GMRES iterations significantly.
- **Smoothing properties and overall multigrid performance** (Table 9 and Figure 7): Here we further analyze the different preconditioners and consider two different coarse grids applied to the four-lobed flower. We see that the Picard preconditioner does the best job of eliminating the high frequencies at multiple resolutions. However, at low resolutions, the Picard smoother is divergent and the resulting preconditioner is ineffective. The FMM-based smoothers are convergent and the resulting preconditioner reduces the total number of GMRES iterations. We also demonstrate that post-smoothing does not sufficiently reduce the number of GMRES iterations to justify its use.
- **Single-grid preconditioners for unresolved geometries** (Table 10): We assess the single-grid preconditioners for two problems. A strategy that couples a Picard two-grid preconditioner with a single-grid FMM-based preconditioner is outlined. We apply several preconditioners to the 8-lobed and 24-lobed flowers. We see that FMMSCHUR preconditioner  $P_{S,1}$  works best which indicates that it is important to include part the far field in the preconditioner, even if it is a very crude low-rank approximation.

Other details of our results include:

- We consider solving (6) for the four geometries in Figure 2. These geometries are selected so that the number of points required to represent the geometry range from a few hundred to several thousands of points.
- Our implementation is in MATLAB. Some of the operators and factorizations are not computed by fast algorithms, so the actual wall-clock times are not informative. For example, all low-rank approximations are computed by truncating MATLAB’s exact SVD to the desired rank. All factorizations of the preconditioners are exact unless otherwise noted. When we use incomplete factorizations, we use MATLAB’s incomplete LU factorization (ILU) with a drop tolerance of  $10^{-3}$ . To compare the different methodologies, we estimate the cost of the preconditioner in terms of the cost to apply  $D$  using the FMM.
- In all of our runs, we use GMRES without restarts preconditioned with the single-grid schemes we discussed in section 3 and V-cycle multigrid. GMRES is terminated when the relative tolerance dropped below  $10^{-12}$ . In

practice, there is no reason to have an algebraic error that is smaller than the truncation error. But for simplicity, we keep the GMRES tolerance fixed in all of our tests.

- In GMRES, we always use the exact double-layer potential; that is, we do not use any FMM approximation. FMM is used only to build the preconditioners. In all runs, unless otherwise stated, we only use four moments for the upward, downward, and translation operators. That is, the far field is approximated with four degrees of freedom per box. In this way, the far field is approximated as crudely as possible within the FMM context.
- For the preconditioners  $P_\ell$ , we have results with  $s = 4$ ,  $s = 10$ , and  $s = 50$  points per leaf. Although we refer to  $P_1$  as including the  $V_1$ -list interactions, it also includes other interactions since the trees are adaptive (Figure 3 and 5). In particular,  $P_1$  also includes the interactions due to the  $W$ -list and  $X$ -list, where these lists are defined in [30].
- For the preconditioner  $P_{S,1}$ , we use a rank five approximation for  $D_1 = L_1 M_1^T$  and for the Schur complement  $M_1^T P_0 L_1$ , and a rank  $5 \log(N/s)$  approximation for  $Z = A - A_0$ . We have conducted experiments for  $P_{S,1}$  where we set  $P_0$  with an ILU factorization of  $A_0$ . We discuss this further in section 4.4.
- Additional parameters include the number of pre- and post-smoothing steps and the number of levels. Results are presented for single-grid, two-grid, and multigrid preconditioners.

**Estimation of the preconditioner cost.** Before we present the results in detail, we discuss how we estimate the cost of each preconditioner. We report the number of scaled matvecs required by our unpreconditioned and different preconditioned runs. These are scaled assuming that the matrix  $D$  can be applied in linear time. For  $P_B, P_D, P_0$ , and  $P_1$ , we assume that their application costs the same as a matvec with  $D$ . Since  $P_B$  and  $P_D$  have a predictable structure, they can be applied efficiently with standard banded and block diagonal solvers. However, our assumption for  $P_0$  and  $P_1$  is quite strong since they require exact factorizations of a sparse but unstructured matrix. Fortunately, an ILU decomposition of  $P_0$ , which can be computed in linear time, can be used without any major effect on the quality of the preconditioner. Concerning  $P_1$ , its exact factorization is impossible and this motivates the single-grid preconditioner  $P_{S,1}$ . The cost of applying  $P_{S,1}$  is  $\mathcal{O}(N \log N)$  since we need to approximate  $Z$ . For the cost of multigrid see section 4.2.

#### 4.1 Single-grid and two-level multigrid, Table 4

We start by comparing single-grid and two-grid preconditioners for all four geometries. For the two-grid preconditioner, we consider two different coarse grids:

$N = 2048$			
Preconditioner	Single-Grid	$N_{\min} = 128$	$N_{\min} = 16$
Picard	16	3	13
$P_D$	16	8	13
$P_0$	16	8	13
$P_1$ -Exact	15	8	13
$P_1$	15	8	13
$P_2$	14	7	12
$P_{S,1}$	7	-	-

$N = 2048$			
Preconditioner	Single-Grid	$N_{\min} = 128$	$N_{\min} = 16$
Picard	26	13	33
$P_D$	27	15	31
$P_0$	25	15	29
$P_1$ -Exact	20	11	17
$P_1$	20	11	17
$P_2$	17	10	14
$P_{S,1}$	9	-	-

$N = 2048$			
Preconditioner	Single-Grid	$N_{\min} = 128$	$N_{\min} = 16$
Picard	42	55	55
$P_D$	44	46	55
$P_0$	30	25	31
$P_1$ -Exact	23	15	23
$P_1$	23	15	23
$P_2$	18	13	19
$P_{S,1}$	10	-	-

$N = 4096$			
Preconditioner	Single-Grid	$N_{\min} = 128$	$N_{\min} = 16$
Picard	115	190	179
$P_D$	99	140	125
$P_0$	55	70	60
$P_1$ -Exact	39	33	47
$P_1$	39	33	47
$P_2$	27	26	41
$P_{S,1}$	19	-	-

Table 4: The number of GMRES iterations required to solve (6) for the four different geometries and several different preconditioners. Top-down we have “Simple”, “Moderate”, “Four-lobed”, and “Eight-lobed” shapes (Figure 2). The numbers reported use the exact factorization for  $P_D$ ,  $P_0$ , and  $P_1$ -Exact. The numbers reported for  $P_1$  and  $P_2$  approximated the terms in  $D_1$  and  $D_2$  with rank four matrices. For  $P_{S,1}$ , we only report single-grid results. Recall that  $P_{S,1}$  is an approximation of  $P_1$  plus a low-rank approximation of  $D_\ell$ ,  $\ell > 1$  interactions. However, if we replace this factorization with a drop-tolerance ILU, the numbers for  $P_{S,1}$  remain unchanged (see Table 10). In the right column, we depict the convergence history of GMRES for some of the cases reported in this table.

$N_{\min} = 128$  and  $N_{\min} = 16$ . The two-grid method uses one pre-smoothing step, followed by a coarse grid solve, and then a prolongation to the fine grid; no post-smoothing steps are used. In these experiments the coarse-grid operators have been constructed using geometry-based coarsening.

The single-grid ‘‘Picard’’ preconditioner is identical to solving (6) with unpreconditioned GMRES. We report results for our new FMM-based preconditioners using exact factorizations of the block diagonal ( $P_D$ ),  $U$ -list ( $P_0$ ), and  $V_1$ -list ( $P_1$ -Exact) preconditioners. The preconditioner  $P_1$ -Exact uses the exact factorization of the double-layer that includes interactions from the  $U$ -list and  $V_1$ -list, whereas  $P_1$  approximates the  $V_1$ -list interactions with FMM compression. The preconditioner  $P_2$  includes the  $U$ -list the compressed  $V_1$ -list and the compressed  $V_2$ -list interactions.<sup>1</sup> Also, we report results for the new FMMSCHUR preconditioner ( $P_{S,1}$ ) which includes a compressed version of the far field. In all cases we use no more than  $s = 10$  points to construct the FMM tree. For  $N = 2048$  this results in 10–11 tree levels. The results are summarized in Table 4. In the rightmost column we plot the relative residuals of the GMRES iterates for a selection of the preconditioners.

For the single-grid results, we observe that introducing more interactions reduces the number of iterations. It is especially important to include some form of the far field as seen by the results for  $P_{S,1}$  which is the most effective. Notice that, by comparing the numbers for  $P_1$  and  $P_1$ -Exact, using FMM compression has little impact on the effectiveness of the preconditioner. For nice geometries like the ‘‘simple’’ and ‘‘moderate’’, which are nearly fully resolved and the number of unpreconditioned GMRES iterations is already small enough, the near field preconditioners  $P_D$ ,  $P_0$ ,  $P_1$  and  $P_2$  have little effect.

The block diagonal preconditioner  $P_D$  is easy to invert, but it does not significantly speedup GMRES. However, using  $P_0$ , the number of GMRES iterations decreases for the flower geometries. Continuing with  $P_1$ , the number of GMRES steps is further reduced. While  $P_1$  is expensive to factor exactly,  $P_{S,1}$ , which approximates  $P_1$  and the remaining far field, is an effective preconditioner. We also report results for  $P_2$  using the same compression that is used for  $P_1$ . As expected, the number of GMRES iterations continues to reduce. One could also approximate  $P_2$  with  $P_{S,2}$  which would require four applications of  $P_0$ .

For the multigrid case, we see that for the ‘‘simple’’ and ‘‘moderate’’ geometries, the two-grid Picard preconditioner with  $N_{\min} = 128$  gives the best results. However, for the other geometries, the Picard preconditioner actually increases the number of GMRES iterations. This is a result of the coarse grid operator being unresolved. The coarse grid  $N_{\min} = 16$  is far too coarse for all the examples and none of our preconditioners are useful. A preliminary conclusion is that using two-grid preconditioner when the coarse grid is unresolved is not effective. A natural question is whether we can improve the coarse grid solver

---

<sup>1</sup>To construct  $P_1$  and  $P_2$ , we have used a crude approach in which we define the approximate matvecs as  $I + D_0$  plus FMM-compressed  $V_1$  plus FMM-compressed  $V_2$ , we build the corresponding sparse matrix using  $N$  multiplications with the columns of the identity matrix, and finally we factorize it exactly to build the corresponding preconditioner. The matrices from the  $V_1$ -list and  $V_2$ -list are approximated with rank four matrices.



by considering alternative coarse operators. We consider this question in our next experiment.

## 4.2 Geometric versus projection coarsening, Tables 5–8

Here we investigate the difference between the two coarse grid operators. We recall that the geometry-based coarse grid operator is formed by restricting the geometry to the coarse grid and then constructing the double-layer potential using the trapezoid rule. The projection-based coarse grid operator is formed by right-multiplying the fine grid operator by the prolongation operator and left-multiplying by the restriction operator. The number of GMRES steps and matvecs (parenthetic values) are reported in Tables 5–8.

We use a standard V-cycle with three levels and one pre- and one post-smoothing step. For the geometry-based coarse grid operators, we require 1.5 matvecs for the pre-smoothing, and therefore, we can estimate the work as three matvecs per V-cycle. For the geometry-based coarse grid we ignore the cost of solving the coarse grid problem. For the projection-based coarse grid operator, we require four matvecs to do pre- and post-smoothing. We also have to add in the cost of doing the coarse grid solve since it requires matvecs with the fine grid operator. We assume that we solve the coarse grid problem with  $m_{\text{coarse}}$  GMRES iterations. Then, the total number of matvecs for a V-cycle with the projection-based coarse grid operator is  $4 + m_{\text{coarse}}$ . We add an additional operation to both methods to account for the single matvec that GMRES requires to compute the residual at each iteration.

For the FMM-based preconditioners, there are  $s = 4$  points per leaf for Tables 5 and 6 and  $s = 10$  points per leaf for Tables 7 and 8. In parenthesis, we report our estimate of the total cost of the method in terms of matvecs with  $D$ . We can immediately see that the projection-based coarse grid operators are far too expensive to apply. Therefore, projection based operators will not be considered any further.

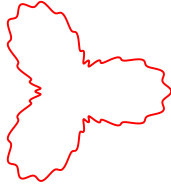
When using the geometry-based coarse grid operator, since the Picard smoother requires no inversions, the banded and block diagonal preconditioners are not able to outperform the Picard smoother. However, for the flower geometries,  $P_0$  and  $P_1$  significantly reduce the number of GMRES iterations. Unfortunately, considering the cost of solving the coarse grid and applying the smoothers, we anticipate that unpreconditioned GMRES will outperform most of the  $V(1, 1)$ -cycles.

Alternatively, we can eliminate the post-smoothing step as we did in the last section and use a  $V(1, 0)$ -cycle. This of course increases the total number of preconditioned GMRES iterations, but it reduces the total number matvecs. This is discussed more in the next section.



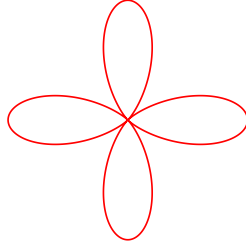
Preconditioner	Geometric	Projection
None	16 (16)	—
Picard	5 (20)	4 (92)
$P_B(2)$	5 (20)	6 (138)
$P_B(10)$	4 (16)	6 (138)
$P_D$	6 (24)	5 (115)
$P_0$	5 (20)	5 (115)
$P_1$	4 (16)	4 (92)

Table 5:  $N = 128$ ,  $N_{\min} = 32$ ,  $m_{\text{coarse}} = 19$ .



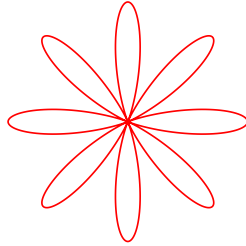
Preconditioner	Geometric	Projection
None	28 (28)	—
Picard	12 (48)	7 (147)
$P_B(2)$	10 (40)	12 (252)
$P_B(10)$	6 (24)	8 (168)
$P_D$	11 (44)	9 (189)
$P_0$	8 (32)	7 (147)
$P_1$	6 (24)	5 (105)

Table 6:  $N = 256$ ,  $N_{\min} = 64$ ,  $m_{\text{coarse}} = 17$ .



Preconditioner	Geometric	Projection
None	42 (42)	—
Picard	21 (84)	4 (96)
$P_B(2)$	21 (84)	12 (288)
$P_B(10)$	20 (80)	17 (408)
$P_D$	21 (84)	7 (168)
$P_0$	12 (48)	5 (120)
$P_1$	9 (36)	5 (120)

Table 7:  $N = 2048$ ,  $N_{\min} = 512$ ,  $m_{\text{coarse}} = 20$ .



Preconditioner	Geometric	Projection
None	115 (115)	—
Picard	111 (444)	12 (312)
$P_B(2)$	148 (542)	30 (780)
$P_B(10)$	75 (300)	52 (1352)
$P_D$	77 (308)	39 (1014)
$P_0$	18 (72)	6 (156)
$P_1$	19 (76)	7 (182)

Table 8:  $N = 4096$ ,  $N_{\min} = 1024$ ,  $m_{\text{coarse}} = 22$ .

### 4.3 Smoothing properties and overall multigrid performance, Table 9

Here we take a closer look at the properties of different preconditioners. First, the Picard preconditioner is guaranteed to have a unit spectral radius as  $N \rightarrow \infty$ . Moreover, it does a great job of quickly eliminating error in the high frequencies. However, if  $N$  is too small the spectral radius is greater than 1 and the scheme diverges. In Figure 7, we consider the four-lobed flower, and we plot the spectrum of the error after one application of several preconditioners for three different values of  $N$ . For all the values of  $N$ , the Picard smoother quickly reduces the error in the high frequencies. However, the spectral radius is greater than 1, and for the smaller values of  $N$ , this leads to poor performance of the multigrid preconditioner. There are cases where our new smoothers also introduce errors in the low frequencies, but their spectral radius is less than one. For instance, for  $N = 512$ , the preconditioner  $P_1$  is convergent, and for  $N = 128$ , all the FMM-based smoothers are convergent.

Figure 7 again shows the importance of resolving the coarse grid operator. If using the Picard preconditioner at too coarse of a grid, the convergence of the preconditioner is poor. However, the FMM-based preconditioners are convergent at these grids.

$N$	$\ D_N 1(\mathbf{x}) + 1/2(\mathbf{x})\ _2$	$Unpre$	<i>Single-Grid</i>	<i>2-Grid</i>		<i>Multigrid</i>	
			$P_0$	Picard	$P_0$	Picard	$P_0$
512	6.6E-2	64	—	—	—	—	—
1,024	1.2E-2	53	35	47	8	47	8
2,048	7.2E-4	42	21	38 (16)	13 (9)	33 (16)	9 (9)
4,096	3.3E-6	41	23	37 (16)	13 (9)	23 (15)	9 (8)
8,192	8.0E-11	41	29	37 (16)	13 (10)	20 (13)	8 (7)

Table 9: The number of unpreconditioned GMRES iterations ( $Unpre$ ) and the number of preconditioned GMRES iterations. Results for a single-grid, two-grid, and multigrid preconditioner are reported. Also reported is an estimate of the  $L^2$ -discretization error. The only preconditioners we consider are Picard and  $P_0$ . Each leaf contains no more than  $s = 50$  points. The values not in parentheses used  $N_{\min} = 512$  whereas those in parentheses used  $N_{\min} = 1024$ .

In Table 9, we consider the four-lobed flower with a coarse grid of  $N_{\min} = 512$  and  $N_{\min} = 1024$ . We increase the number of points per leaf to  $s = 50$ . We compare the Picard preconditioner with  $P_0$  and consider single-grid, two-grid, and a standard V-cycle multigrid. We only use one pre-smoothing step since there is not a justification for a post-smoothing step after considering the small reduction in the GMRES iterations (numbers not reported).

We see that with  $N_{\min} = 512$ ,  $P_0$  creates better two-grid and multigrid preconditioners. This is consistent with Table 7. However, if the coarse grid is refined to  $N = 1024$  (parenthetic values), the Picard preconditioner improves dramatically while  $P_0$  only has a slight improvement. Again, we are observing

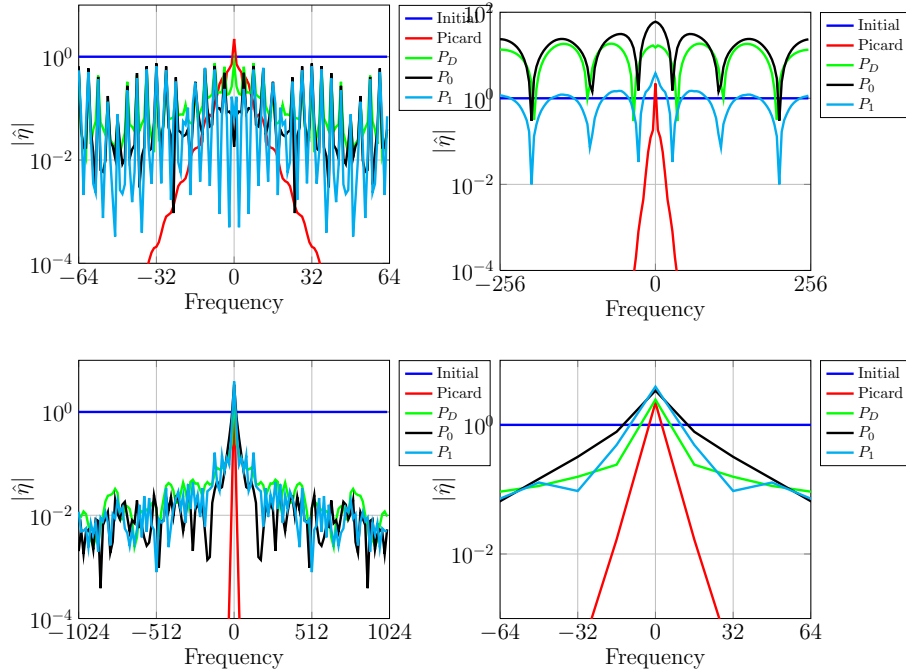


Figure 7: The error after one iteration of smoothers based on Picard,  $P_D$ ,  $P_0$ , and  $P_1$ . The geometry is the four-lobed flower with  $N = 128$  (top-left),  $N = 512$  (top-right), and  $N = 2048$  (bottom) points. The bottom-right plot is a zoomed in copy of the bottom-left plot. We set the right-hand side to  $f = 0$  and start with an initial guess that is the sum of all the Fourier frequencies. We see that the Picard preconditioner does a much better job of quickly eliminating the high frequencies in the error. However, for  $N = 128$ , it is divergent while the other three smoothers are convergent. While these three smoothers do not do as good of a job at eliminating the high frequencies, we have seen that they create better preconditioners than the Picard preconditioner at low resolutions.

that our new FMM-based preconditioners only payoff if the coarsest grid is sufficiently coarse; at these resolutions, the Picard preconditioner fails. Also reported are the number of single-grid preconditioned steps and an estimate of the discretization error at all the resolutions.

Assuming that the coarse grid is resolved, the Picard smoother outperforms our new FMM-based smoothers. However, the coarse grid operator still needs to be inverted using an iterative method since it can be too large for an exact factorization. This is where we envision our new FMM-based preconditioners playing a role. That is, we use a standard V-cycle with the Picard preconditioner, but the coarse grid operator is preconditioned with an FMM-based preconditioner. We discuss this in more detail in the next section.

#### 4.4 Single-grid preconditioners for unresolved geometries, Table 10

8-lobed flower						
$N$	$\ D_N \mathbf{1}(\mathbf{x}) + 1/2(\mathbf{x})\ _2$	$Unpre$	$P_D$	$P_0$	$P_1$	$P_{S,1}$
512	2.7E-1	141	56	20 (21)	9	6 (6)
1,024	1.0E-1	205	68	26 (28)	13	6 (7)
2,048	3.3E-2	255	112	26 (28)	17	8 (8)
4,096	6.2E-3	145	108	36 (39)	23	10 (11)
8,192	3.6E-4	108	103	30 (31)	17	8 (8)
24-lobed flower						
$N$	$\ D_N \mathbf{1}(\mathbf{x}) + 1/2(\mathbf{x})\ _2$	$Unpre$	$P_D$	$P_0$	$P_1$	$P_{S,1}$
512	1.8E+0	250	125	34 (38)	12	9 (9)
1,024	8.5E-1	239	120	25 (28)	12	11 (11)
2,048	4.0E-1	328	151	37 (39)	20	16 (17)
4,096	1.8E-1	444	112	56 (59)	29	20 (21)
8,192	7.8E-2	578	166	62 (66)	35	24 (25)
16,384	2.8E-2	730	221	81 (83)	43	29 (29)

Table 10: Here we report the number of unpreconditioned ( $Unpre$ ) and the number of preconditioned GMRES iterations. We report results for a single-grid, with several preconditioners. Recall that,  $P_D$  is a block diagonal preconditioner, where we invert the box interactions,  $P_0$  is based on factorizing the direct interactions (U-list),  $P_1$  is based on factorizing the direct plus the first level of far interactions ( $U$ -list +  $V_1$ -list), and  $P_{S,1}$  is an approximation of  $P_1$  plus an approximation of the remaining far interactions. To show how well we have discretized the geometry we give the  $L^2$ -discretization error for a unit density. The results in parentheses are obtained by replacing the exact factorization of  $P_0$  with an ILU factorization with a drop tolerance of  $10^{-3}$ . For both shapes we used  $s = 50$ . Recall that we estimated the cost of  $P_{S,1}$  to two matvecs and the cost of  $P_0$  to one matvec.

We have observed that if the coarse grid is resolved, the Picard smoother

quickly eliminates the high frequencies (Figure 7) and the resulting two-grid  $V(1,0)$ -cycle is an effective preconditioner. However, for complex geometries, the coarse grid operator is too large to solve directly. We now investigate preconditioning the coarse grid operator with a single-grid FMM-based preconditioner.

In Table 10, we consider the 8-lobed flower and a 24-lobed flower (see Figure 1). We compute the required number of GMRES steps to converge to a random right-hand side with the single-grid preconditioners  $P_D$ ,  $P_0$ ,  $P_1$ , and  $P_{S,1}$ . Moreover, we test inexact factorizations of  $P_0$  by using the incomplete LU factorization with a drop tolerance of  $10^{-3}$  (parenthetic values).

For these complex geometries,  $P_D$  and  $P_0$  are not able to significantly reduce the number of GMRES steps. However  $P_1$  and especially  $P_{S,1}$  do result in a significant reduction. This indicates that including part of the far field, even if it is a low-rank approximation, drastically improves the quality of the preconditioner. Moreover, using the ILU factorization of  $P_0$  when applying  $P_{S,1}$  results in a negligible increase in the number of GMRES iterations.

## 5 Conclusions

Let us summarize the conclusions we drew from the numerical experiments.

- Multigrid preconditioners are only effective if the geometry has adequate resolution at the coarsest grid. Moreover, the layer potential must be approximated geometrically, not with projections. Therefore, if we need  $N_\eta$  points to accurately resolve  $\boldsymbol{\eta}$  and  $N$  points to resolve the geometry, and  $N_\eta > N$ , then multigrid pays off.
- For smoothing we can use either Picard or  $P_0$ -based split stationary solver.
- For problems with multiple regions of high curvature, the coarse grid may require a quite large value for  $N$  meaning that a direct factorization is too expensive. Therefore, we need single-grid preconditioners. Everything else is likely to be too expensive.
- For the coarse-grid, the FMMSCHUR preconditioner  $P_{S,1}$  seems to be the best choice for GMRES.
- The cost effectiveness of these schemes relies on our ability to construct  $P_0$  using a fast factorization of  $A_0$ . We tested incomplete factorizations and we found that these have little effect to the overall performance of the preconditioners. Therefore, we can use one of the available parallel approximate sparse factorization methods. But for real scalability, further research is required for the efficient factorization of the near field interactions.

In all of our results we have used a small number of points per leaf (10–50). Typically in the FMM, the number is bigger and is chosen to minimize the constants in the complexity. Here we have chosen it so that the FMM trees

are quite deep and a significant part of the interactions is not captured in the factorizations. For example, for  $N = 4,096$  we end up with 12 tree levels. That means most of the far field is captured only by the low-rank approximation of  $Z$ .

For problems with stationary boundaries, one often has to solve the same integral equation for multiple right-hand sides. This is the case when discretizing a time-dependent problem in time and then using an integral equation method to solve the resulting spatial problem. In these problems, it is often advantageous to precompute approximate inverses or preconditioners that can be quickly applied to these right-hand sides. The cost of constructing the preconditioners is important, particularly for problems with a small number of right-hand sides per solve. Such cases include shape optimization, inverse problems, or moving boundary problems in fluid mechanics. We estimate that in an optimal implementation the construction complexity will be  $\mathcal{O}(N \log N)$  but the details are ongoing work.

Overall, assessing the true effectiveness of the preconditioners requires production quality implementations. A well-tuned FMM combined with GMRES and fast direct solvers have reasonably low costs and eventually a preconditioner has to be tested against such an implementation (perhaps preconditioned with cheap methods like block diagonal methods in [11]). Indeed, the effectiveness of numerical schemes for well-conditioned linear systems depends on the constants since all the methods we are discussing are mesh-independent but not geometry-independent (see Table 3).

Finally, we mention that we expect that our preconditioners will not be effective for Helmholtz equations at high frequencies. The matrices corresponding to the  $V_\ell$ -lists are not low-rank and we anticipate that we will be unable to use compression and incomplete factorizations as we have in this paper. However, ideas of this paper can be applied to other PDEs such as the Stokes, the Yukawa, and the biharmonic equations.

## References

- [1] Rainer Kress. *Linear Integral Equations*. Applied Mathematical Sciences. Springer, 1999.
- [2] Yousef Saad and Martin H Schultz. GMRES: A Generalized Minimal Residual Algorithm for Solving Nonsymmetric Linear Systems. *SIAM Journal on Scientific and Statistical Computing*, 7(3):856–869, July 1986.
- [3] L. Greengard and V. Rokhlin. A Fast Algorithm for Particle Simulations. *Journal of Computational Physics*, 73:325–348, 1987.
- [4] N. Halko, P. Martinsson, and J. Tropp. Finding structure with randomness: Probabilistic algorithms for constructing approximate matrix decompositions. *SIAM Review*, 53:217–288, 2011.

- [5] Leslie Greengard, Denis Gueyffier, Per-Gunnar Martinsson, and Vladimir Rokhlin. Fast direct solvers for integral equations in complex three-dimensional domains. *Acta Numerica*, 18(1):243–275, 2009.
- [6] PW Hemker and H Schippers. Multiple grid methods for the solution of Fredholm integral equations of the second kind. *Mathematics of Computation*, 36(153):215–232, 1981.
- [7] Wolfgang Hackbusch. *Multigrid methods and applications*, volume 4 of *Springer Series in Computational Mathematics*. Springer-Verlag, Berlin, 1985.
- [8] H. Schippers. *Multiple Grid Methods For Equations of the Second Kind With Applications in Fluid Mechanics*. PhD thesis, University of Technology Delft, 1982.
- [9] A. Brandt and A. A. Lubrecht. Multilevel matrix multiplication and fast solution of integral equations. *Journal of Computational Physics*, 90(2):348–370, October 1990.
- [10] Kendall E. Atkinson. Two-Grid Iteration Methods For Linear Integral Equations of the Second Kind on Piecewise Smooth Surfaces in  $\mathbb{R}^3$ . *SIAM Journal on Scientific Computing*, 15(5):1083–1104, September 1994.
- [11] K. Nabors, F. T. Korsmeyer, F. T. Leighton, and Jacob K. White. Preconditioned, adaptive, multipole-accelerated iterative methods for three-dimensional first-kind integral equations of potential theory. *SIAM Journal on Scientific and Statistical Computing*, 15:713–735, 1994.
- [12] Ananth Grama, Vipin Kumar, and Ahmed Sameh. Parallel hierarchical solvers and preconditioners for boundary element methods. *SIAM Journal on Scientific Computing*, 20(1):337–358, 1998.
- [13] Josh Barnes and Piet Hut. A hierarchical  $O(N \log N)$  force-calculation algorithm. *Nature*, 324(4):446–449, December 1986.
- [14] Ke Chen. An Analysis of Sparse Approximate Inverse Preconditioners for Boundary Integral Equations. *SIAM Journal on Matrix Analysis and Applications*, 22(4):1058–1078, 2000.
- [15] Bruno Carpentieri, Iain S Duff, Luc Giraud, and Guillaume Sylvand. Combining fast multipole techniques and an approximate inverse preconditioner for large electromagnetism calculations. *SIAM Journal on Scientific Computing*, 27(3):774–792, 2005.
- [16] Jeonghwa Lee, Jun Zhang, and Cai-Cheng Lu. Incomplete LU preconditioning for large scale dense complex linear systems from electromagnetic wave scattering problems. *Journal of Computational Physics*, 185(1):158–175, 2003.



- [17] S. K. Veerapaneni, D. Gueyffier, D. Zorin, and G. Biros. A boundary integral method for simulating the dynamics of inextensible vesicles suspended in a viscous fluid in 2D. *Journal of Computational Physics*, 228(7):2334–2353, 2009.
- [18] P. G. Martinsson and V. Rokhlin. A fast direct solver for boundary integral equations in two dimensions. *Journal of Computational Physics*, 205(1):1–23, 2005.
- [19] Phillip G Schmitz and Lexing Ying. A fast direct solver for elliptic problems on general meshes in 2D. *Journal of Computational Physics*, 231(4):1314–1338, 2012.
- [20] Kenneth L Ho and Leslie Greengard. A fast direct solver for structured linear systems by recursive skeletonization. *SIAM Journal on Scientific Computing*, 34(5):A2507–A2532, 2012.
- [21] A. Greenbaum, L. Greengard, and G. B. McFadden. Laplace’s Equation and the Dirichlet-Neumann Map in Multiply Connected Domains. *Journal of Computational Physics*, 105:267–278, 1993.
- [22] P. G. Martinsson. A direct solver for variable coefficient elliptic PDEs discretized via a composite spectral collocation method. *Journal of Computational Physics*, 2013.
- [23] B. Folland. *Introduction to Partial Differential Equations*. Princeton University Press, Princeton, New Jersey, 1995.
- [24] O. D. Kellogg. *Foundations of Potential Theory*. Dover, 1953.
- [25] S. G. Mikhailin. *Integral Equations*. Pergamon Press, New York, 1957.
- [26] Lexing Ying, George Biros, and Denis Zorin. A kernel-independent adaptive fast multipole method in two and three dimensions. *Journal of Computational Physics*, 196(2):591–626, 2004.
- [27] Xiaobai Sun and Nikos P Pitsianis. A matrix version of the fast multipole method. *SIAM Review*, 43(2):289–300, 2001.
- [28] Kendall E. Atkinson. A Survey of Numerical Methods for Solving Nonlinear Integral Equations. *Journal of Integral Equations*, 4(1), 1992.
- [29] Kendall E. Atkinson. *The Numerical Solution of Integral Equations of the Second Kind*. Cambridge University Press, 1997.
- [30] J. Carrier, L. Greengard, and V. Rokhlin. A Fast Adaptive Multipole Algorithm for Particle Simulations. *SIAM Journal on Scientific and Statistical Computing*, 9(4):669–686, 1988.